

LiDAM: Semi-Supervised Learning with Localized Domain Adaptation and Iterative Matching

Qun Liu, Matthew Shreve, and Raja Bala

Palo Alto Research Center
Palo Alto, California

Abstract

Although data is abundant, data labeling is expensive. Semi-supervised learning methods combine a few labeled samples with a large corpus of unlabeled data to effectively train models. This paper introduces our proposed method LiDAM, a semi-supervised learning approach rooted in both domain adaptation and self-paced learning. LiDAM first performs localized domain shifts to extract better domain-invariant features for the model that results in more accurate clusters and pseudo-labels. These pseudo-labels are then aligned with real class labels in a self-paced fashion using a novel iterative matching technique that is based on majority consistency over high-confidence predictions. Simultaneously, a final classifier is trained to predict ground-truth labels until convergence. LiDAM achieves state-of-the-art performance on the CIFAR-100 dataset, outperforming FixMatch (73.50% vs. 71.82%) when using 2500 labels.

1 Introduction

Although the amount of data being generated is increasing every year (Mittal and Sangwan 2019), most of this data is unlabeled. Acquiring labels to sufficiently train fully supervised models is often prohibitively expensive and time-consuming. Given that data-driven deep networks require millions of labeled samples to train, there is a growing interest in semi-supervised methods that learn from a combination of a few labeled samples and a large quantity of unlabeled data (Berthelot et al. 2019b; 2019a; Sohn et al. 2020).

We focus on the task of deep image classification. A fundamental component of semi-supervised learning is the detection of clusters that form in the feature projections of unlabeled data. These clusters are assigned pseudo-labels that, when combined with a handful of real labels, can be used to train and update the classifier. The ultimate goal is to group samples together by propagating real labels to nearby samples with a high degree of confidence. In fact, it was recently shown that iteratively applying a combination of clustering and supervised learning (using only pseudo-labels) on a randomly initialized model can achieve remarkable accuracy for image classification (Caron et al. 2018). In our work,

we adopt a similar approach but push performance further by borrowing concepts from transfer learning, and domain adaptation. Additionally our method takes as input initial feature representations from a pretrained or a self-supervised model that requires no human-annotated labels (e.g., MoCo (He et al. 2019) or SimCLR (Chen et al. 2020)).

Our work is in large part motivated by the observation that many large datasets, especially those collected from on-line scraping algorithms (e.g., CIFAR, ImageNet, etc.), exhibit high intra-class variance due to diversity in the domains from which the images arise. For example, images within a given class may be sourced from official product advertisements, low quality mobile captures for social networking, images captured from surveillance feeds at oblique poses, etc. In addition intra-class shifts can also arise from regional trends (e.g., images of different dog breeds popular within different populations, but all labeled *dog*). Our hypothesis is that by explicitly modeling intra-class domain variance using localized domain adaptation, we improve the likelihood that clusters align with true classes.

We propose a two-stage approach as shown in Figure 1. In the first stage, we begin by generating feature representations from the unlabeled images using a pretrained or self-supervised model. We then apply K -means clustering and assign a pseudo-label to each sample based on the cluster ID. For each cluster, a *centricity-based* confidence measure is used to extract a subset S_c of samples from which two data subsets are selected corresponding to a source and target domain, denoted S_s and S_t . Next, a generative domain adaptation model (DAM) is trained to learn domain-invariant feature representations and to predict pseudo-labels in a space with compact clusters. This is followed by an initial alignment between true and pseudo-labels, achieved by feeding labeled samples to DAM, and assigning true labels to all unlabeled data via a *majority consistency* rule. In the second stage, we perform a proposed *self-paced iterative matching* technique to train the final classifier to predict true class labels for all unlabeled samples.

Our novel contributions are twofold: i) the use of deep domain adaptation on artificially induced domain shifts to generate high-quality initial data representations and labels; and ii) introduction of a novel iterative scheme to simultane-

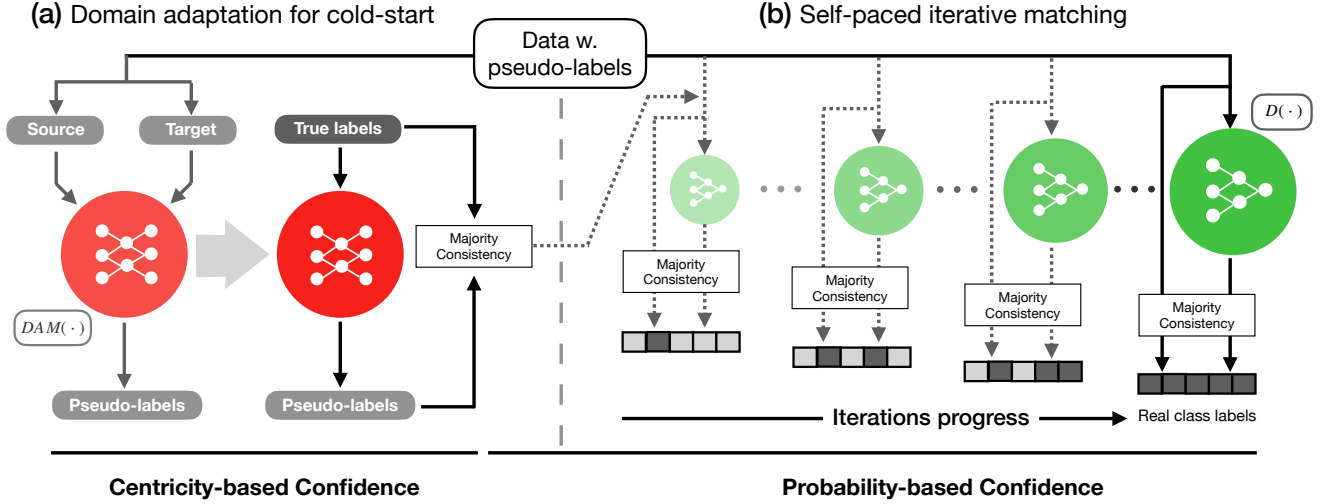


Figure 1: Overview of proposed two-stage method. In stage (a), feature points and pseudo-labels from K -means are used to train the Domain Adaptation Model (DAM, red circle). DAM generates an initial prediction of class labels, which are fed to stage (b) where labels and the classifier (green circle) are iteratively updated until convergence. Iterations are shown unrolled for illustration (figure best viewed in color).

ously update data labels and the final classifier.

Our experimental results demonstrate that our method can align pseudo-labels to ground-truth labels with a high degree of accuracy. Overall, our method achieves competitive performance on both the CIFAR-10 and CIFAR-100 datasets under the same semi-supervised setting. On the CIFAR-100 dataset, we outperform the state-of-the-art (73.50% vs. 72.88%) when only using 5% of the available labels, while outperforming the majority of methods when a larger number of labels is used. To the best of our knowledge, LiDAM is the first approach that combines unsupervised clustering with localized domain adaptation and an iterative matching mechanism to generate accurate pseudo-labels.

2 Related work

Domain adaptation and transfer learning Recently, adversarial learning has been used to improve the marginal and conditional distributions of cross-domain sample populations for the purpose of transfer learning (Yu et al. 2019; Zhao et al. 2018). Such approaches jointly train a feature generator (G_f) and discriminator (G_d) so that the final distributions between the source and target domains are as close as possible, resulting in a domain invariant set of features. (Lee et al. 2019) improves on this idea by proposing an additional filter that ignores portions of visual data that do not transfer well through the use of a *residual transferability aware bottleneck*. Alternatively, negative and positive transfer measures can determine how effective features learned for some previous task transfer to a new target task. In the work by (Cao et al. 2018), these measures are explored on each class separately to determine if a class should be learned in the source domain and if so, how it should be weighted in a transfer process. In contrast to these approaches which seek to globally adapt inter-class features

across two domains, we *locally* adapt features for each class to suppress intra-class domain variances.

Semi-supervised learning While a comprehensive survey of the semi-supervised learning literature is beyond scope, here we highlight a few techniques related to our approach. The sample-efficient method proposed in (Lee 2013) assigns pseudo-labels to unlabeled data for classes that are predicted with high probability. These labels are then aligned with true labels using a majority rule to train a network in a supervised fashion. The MixMatch algorithm by (Berthelot et al. 2019b) proposes using low-entropy labels for unlabeled data. Their approach also combines augmented data with labeled data to predict the classes of unlabeled data. This technique was improved in ReMixMatch (Berthelot et al. 2019a) by aligning the distributions of augmentation anchoring techniques, to align marginal distributions between predictions of unlabeled data and true labels, and to align the output of strongly augmented inputs with that of weakly augmented ones. The same authors (Sohn et al. 2020) proposed FixMatch that combines consistency regularization and pseudo-labeling to align the predictions of pseudo labels between weakly and strongly augmented unlabeled images. Our approach is different from these methods in that we initiate our model with a novel combination of unsupervised clustering and localized domain adaptation, and then align pseudo-labels to true labels using a new iterative matching algorithm.

3 Method

We describe in detail our proposed LiDAM approach.

3.1 Unsupervised Clustering

We perform K -means clustering on features extracted from each image and assign an initial pseudo-label prediction

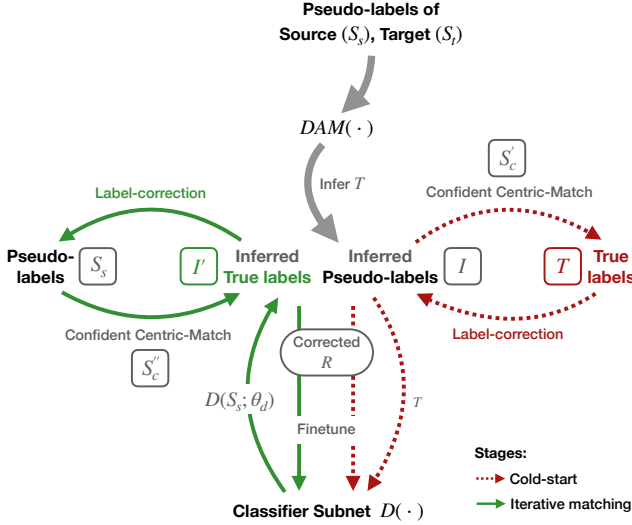


Figure 2: Detailed illustration of our proposed approach. A domain adaptation model trained on pseudo-labels is initially used to predict real class labels for an unlabeled dataset T , solving the cold start problem (dashed loops in red). These predictions are then used initially train a separate classifier D that is iteratively updated using alternating label mapping mechanisms (solid green loops).

based on cluster ID. Rather than cluster on features from a randomly initialized model as performed in (Caron et al. 2018), we cluster on the feature space generated from either a model pretrained on a different dataset, or one trained using a self-supervised learning pretext task (He et al. 2019). Next we select from the dataset two subsets that we treat as arising from separate domains. The selection is based on two premises: the first is that compact groups of samples that tightly surround each cluster’s mean location are more likely belong to the same class, as demonstrated in (Garg and Kalai 2017). The second is based on our hypothesis that these points also belong to the same domain. Conversely, points withing each cluster that are far away from the cluster mean are more likely to belong to a different class and also very likely belong to a different domain. These subsets are then used to train a deep Domain Adaption Model (DAM) to learn domain-invariant features that lead to more compact class clusters, and accurate pseudo-label predictions.

3.2 Domain Adaptation Model

We adopt the adversarial domain adaption strategy described in (Ganin and Lempitsky 2015). This architecture comprises 3 subnets. First, a subnet $M(\cdot)$ with parameters θ_m learns domain-invariant feature representations. These are fed to both a domain discriminator $G(\cdot)$ with parameters θ_g that distinguishes between source and target domain; and a classifier $C(\cdot)$ with parameters θ_c that predicts class labels. Training proceeds as a two-player *minmax* game that simultaneously maximises the loss \mathcal{L}_g of $G(\cdot)$ (encouraging domain-invariant features) while minimizing the loss \mathcal{L}_c of

$C(\cdot)$ (maximizing classification accuracy). The overall network loss is given by:

$$\mathcal{L}_{ori}(\theta_m, \theta_c, \theta_g) = \frac{1}{N_s} \sum_{i=1}^{N_s} \mathcal{L}_c(y_i, C(M(X_i))) - \frac{\lambda}{N} \sum_{j=1}^N \mathcal{L}_g(l_j, G(M(X_j))) \quad (1)$$

where X_i and y_i are input images and pseudo-labels respectively, N_s and N_t are the number of samples in the source and target domains respectively, and N is the total dataset size. Hyperparameter λ balances the importance of classifier loss \mathcal{L}_c vs. domain discriminator loss \mathcal{L}_g . The binary variable $l_j \in \{0, 1\}$ denotes whether a sample is from the source or target domain. Network parameters are learned through the *min-max* optimization shown below,

$$\begin{aligned} (\hat{\theta}_m, \hat{\theta}_c) &= \arg \min_{\theta_m, \theta_c} \mathcal{L}_{ori}(\theta_m, \theta_c, \theta_g), \\ (\hat{\theta}_g) &= \arg \min_{\theta_g} \mathcal{L}_{ori}(\theta_m, \theta_c, \theta_g). \end{aligned} \quad (2)$$

Since the overall number of domains present in each class is unknown, we do not know *a priori* the class overlap between source and target domains. Hence, we adopt a partial domain adaptation technique. In general, aligning the source label space L_s to the target label space L_t can result in classification performance decay due to effects from the outlier label space $L_s \setminus L_t$ of source labels that are not represented in the target domain. We assume a common scenario where $|L_t| \ll |L_s \setminus L_t|$ (this is reflected in our choice of source and domain set sizes in Section 4). We implement the partial adversarial domain adaptation approach defined in (Cao et al. 2018) by assigning weights on source domain classes to reduce the interference from outlier classes when learning transferable features. The weight \mathbf{v} is a $|L_s|$ dimensional vector that enhances weights on $L_s \cap L_t$ and attenuates weights on $L_s \setminus L_t$. Specifically, \mathbf{v} quantifies contributions from each class by averaging the label predictions over target data:

$$\mathbf{v} = \frac{1}{N_t} \sum_{i=1}^{N_t} \hat{\mathbf{y}}_i, \quad (3)$$

Note that the weight \mathbf{v} satisfies $\sum_{i=1}^{|L_s|} v_i = 1$. By normalizing the weight \mathbf{v} by its maximum value, $\mathbf{v} / \max(\mathbf{v})$ small weights are assigned to $L_s \setminus L_t$. We apply the weight \mathbf{v} to the classifier $C(\cdot)$ and the discriminator $G(\cdot)$ over source domain data to equations (1) and (2) and define losses for partial domain adaptation:

Algorithm 1: Iterative Matching

```

1 Pretrain( $DAM$ )
2  $DAM(T; \theta_c) \rightarrow I$   $\blacktriangleright$  inferred pseudo-labels
3  $I \rightarrow S'_c$   $\blacktriangleright$  select confident pseudo-label set
4 Initialize( $Loop$ )
5 while  $Acc_L \geq Acc_{best}$  do
6   if  $Model_L$  not exist then
7     for number of classes do
8        $l_{new} = Map(\mathbf{I}^{l_p} \rightarrow \mathbf{T}^{l_t})$   $\blacktriangleright$  match to true labels
9        $Update(R) \leftarrow l_{new}$ 
10    end
11  else
12     $Acc_{best} = Acc_L$ 
13     $Model_{best} = Model_L$ 
14     $D(S_s; \theta_d) \rightarrow I'$   $\blacktriangleright$  inferred true labels
15     $I' \rightarrow S''_c$   $\blacktriangleright$  confident inferred true label set
16    for number of classes do
17       $l'_{new} = Map(\mathbf{S}'_p \rightarrow \mathbf{I}'^{l_t})$   $\blacktriangleright$  match to inferred true labels
18       $Update(R) \leftarrow l'_{new}$ 
19    end
20  end
21  Tune classifier  $D(R; \theta_d)$  and finetune with  $T$ 
22  Save( $Model_L, Acc_L$ )  $\blacktriangleright$  save model, accuracy
23 end

```

$$\begin{aligned}
\mathcal{L}_{par}(\theta_m, \theta_c, \theta_g) = & \frac{1}{N_s} \sum_{i=1}^{N_s} v_{y_i} \mathcal{L}_c(y_i, C(M(X_i))) \\
& - \frac{\lambda}{N_s} \sum_{i=1}^{N_s} v_{y_i} \mathcal{L}_g(l_i, G(M(X_i))) \quad (4) \\
& - \frac{\lambda}{N_t} \sum_{j=1}^{N_t} \mathcal{L}_g(l_j, G(M(X_j)))
\end{aligned}$$

where the hyper-parameter λ is same as defined in equation (1) and v_{y_i} is the weight corresponding to the ground-truth label y_i with source data X_i . The parameters are then learned through *min-max* optimization:

$$\begin{aligned}
(\hat{\theta}_m, \hat{\theta}_c) &= \arg \min_{\theta_m, \theta_c} \mathcal{L}_{par}(\theta_m, \theta_c, \theta_g), \\
(\hat{\theta}_g) &= \arg \min_{\theta_g} \mathcal{L}_{par}(\theta_m, \theta_c, \theta_g). \quad (5)
\end{aligned}$$

3.3 Label initialization

Given an initially pseudo-labeled training set R , we identify a subset of samples S_c for which we have a high degree of confidence in the pseudo-label prediction. This is achieved by selecting the k neighbors nearest to each cluster centroid based on Euclidean distance. S_c is randomly divided into a source domain set S_s and a target domain set

S_t . The value of k is empirically selected to balance pseudo-label and ground-truth label prediction accuracy (explained in more detail in Section 4 and Figure 3).

To start the iterative matching process and address the cold-start problem of predicting ground-truth labels for unlabeled samples, we adopt the following *majority consistency* approach. We run the small set T of labeled samples through $DAM(\cdot)$ to get predicted pseudo-labels. Note that samples from a given true class can map to multiple pseudo-labels. We count the occurrences of pseudo-label predictions within a given true class, and assign to that class the pseudo-label with the majority count. Now every labeled sample has both a true and pseudo label. Next, the loop is closed by reversing this mapping and aligning each pseudo-label with a ground-truth label for all unlabeled samples, as shown in the right half of Figure 2. To this end, we define a function Map that matches pseudo-class label l_p to a true class label $l_t \in [0, Z]$ and returns the true label l_t as correct label l_{new} ,

$$l_{new} = Map(\mathbf{I}^{l_p} \rightarrow \mathbf{T}^{l_t}). \quad (6)$$

To do this, Map first counts the frequency of the ground-truth labels associated with each group of samples that have the same high-confidence pseudo-label prediction from $DAM(\cdot)$. Initially, all high confidence pseudo-label predictions are stored in $S'_c = \{x_i^j | P_r(I_i) \geq 1 - \alpha, i \in 1, 2, \dots, |T|, j \in 1, 2, \dots, Z\}$ where α is a hyper-parameter ($\alpha = 1e-5$ in our experiments). Then, all samples S'_c with the same pseudo-label prediction l_p are collected in the set $\mathbf{x}^{l_p} \in S'_c$. After determining the most frequently occurring ground-truth label l_t , we propagate the ground-truth label to all members of \mathbf{x}^{l_p} by replacing the pseudo-label with the true class label l_t . After each pseudo-class label has been matched and updated in R , we use this newly labeled dataset to train a new classifier $D(\cdot)$ (ResNet-50), which is iteratively finetuned with labeled samples T for downstream classification.

3.4 Iterative matching

After the cold-start initialization using T , classifier $D(\cdot)$ is able to start inferring true class labels I' for the initial source set with high centrality-based confidence scores S_s . During each iteration (denoted as a solid green line in Figure 2), the assigned pseudo-label S_s is updated based on high confidence predictions by $D(\cdot)$. To achieve this, the mapping rule is in the reverse direction as described in Eq. 6 since $D(\cdot)$ predicts true labels as opposed to the pseudo-labels predicted by $DAM(\cdot)$. Thus, Map follows the same process but maps each pseudo-label l'_p of S_s to a true class label l'_t of I' and returns the true class label as the correct label l'_{new} ,

$$l'_{new} = Map(\mathbf{S}'_p \rightarrow \mathbf{I}'^{l_t}). \quad (7)$$

where l'_t is the most frequent inferred true label on $\mathbf{x}^{l'_p}$ with associated pseudo-label l'_p , and $\mathbf{x}^{l'_p} \in S'_c$ and S'_c is an inferred true label set that contains samples with high probability detections from $D(\cdot)$. That is, $S'_c = \{x_i^j | P_r(I_i) \geq$

Table 1: The effect from the size of confident pseudo label set for the performance of Kmeans clustering on CIFAR-10.

Cluster subset $ S_c $	Total correct	K-means acc.
500	4762	0.9524
1000	9326	0.9326
1500	13732	0.9155
2000	18089	0.9045

$1 - \alpha', i \in 0, 1, 2, \dots, |S_s|, j \in 0, 1, 2, \dots, Z\}$ where α' is a hyper-parameter that thresholds predicted confidence values ($\alpha' = 1e-2$ in our experiments). Note that S_s can potentially affect downstream classification performance if the initial K -means clustering performance is poor. Thus, choosing a good size for S_c is critical (we explore different sizes for S_s in our experimental results and in Table 1 and Table 2). Once pseudo-class labels are matched and updated in R with T , we again fine-tune the classifier $D(\cdot)$ and continue iterating. As the number of iterations increase, more and more pseudo-labels will be correctly aligned to true labels (as illustrated in Figure 1-b). The classifier $D(\cdot)$ is thus progressively improved by optimizing the following problem,

$$\arg \min_{\theta_d} \sum_{i=1}^{|R|} \mathcal{L}_d(y_i, D(x_i; \theta_d)) \quad (8)$$

where θ_d is the parameters of classifier $D(\cdot)$ with the loss \mathcal{L}_d for $x_i \in R$. The iterations conclude when the predicted class labels converge with the ground-truth labels for all samples in T ; and the resulting classifier $D(\cdot)$ is used for predicting true labels for all samples. The process is summarized in Algorithm 1.

4 Experiments

We demonstrate the performance of our method on image classification, making comparisons to several state-of-the-art methods. Our experiments are performed on two benchmark image classification datasets, CIFAR-10 and CIFAR-100 (Krizhevsky, Nair, and Hinton 2009) using standard ground-truth partitioning techniques used for measuring semi-supervised learning performance.

4.1 Datasets

CIFAR-10 contains a total of 60000 RGB images from ten classes. The image size is 32×32 and each class has 6000 images. 1000 images from each class are randomly selected to form a test set, while the remaining images are used for training.

CIFAR-100 is similar to CIFAR-10 except with 100 classes, each containing 600 RGB images. 500 images from each class comprised a training dataset of 50000 images and the remainder are used for testing. CIFAR-100 is more challenging as it has much more classes and fewer images for training than CIFAR-10.

Table 2: The effect of the size of confident pseudo label set for the performance of Kmeans clustering on CIFAR-100.

Cluster subset $ S_c $	Total correct	Kmeans acc.
30	1775	0.5917
60	3415	0.5692
90	5052	0.5613
120	6553	0.5461

4.2 Implementation details

Our approach relies on an initial set of feature representations extracted from the images. We use a ResNet-152 pretrained on ImageNet to both extract feature representations for the K -means clustering in the first stage, and as the backbone for the classifier in the second iterative matching stage.

We divide S_c into an 80 / 20 split for the source and target subsets S_s , and S_t respectively. For selecting the number of ground-truth samples used to train our models, we follow standard practice: for CIFAR-10, the test on ground-truth selections sizes of 250, 1000, and 4000 which comprise images randomly selected from each class in groups of 25, 100, and 400, respectively; for CIFAR-100, ground-truth selections of 2500, 5000, and 10000 are comprised by randomly selecting 25, 50, and 100 images per class, respectively. For our reported image classification tests, we use the standard test data partition from CIFAR-10 and CIFAR-100.

4.3 Evaluation

We first evaluate how well K -means clustering performs when choosing the closest N samples around each cluster center (i.e. S_c). As can be seen from Table 1 and Table 2, different choices of N lead to different levels of cluster accuracy or purity (i.e., the number of samples with a common ground-truth label that is unique from other clusters). One clear and intuitive takeaway from both of these results is that as the distance increases from the cluster center, the more likely we are to acquire impurities (i.e. samples of different classes). As discussed in Section 3, this is important for two reasons. The first reason is that since the subset S_c is used for selecting the intra-class source and target domain sets around each cluster which are used to train DAM , any impurity will likely increase inter-class confusion. The second reason is that these samples are expected to be of a singular class when training the final classification model during the iterative matching stage.

To get an insight of how the choice of S_c and its subdivisions S_t , and S_s will effect the training performance of DAM , we conducted a series of experiments as shown in Figure 3. In these experiments, S_t serves as test data except for the experiment shown in Figure 3(c) where we use the standard CIFAR-10 test data partition. We compare two approaches for subdividing S_c into the source (S_s) and target (S_t) domains. In the first approach, each sample is randomly assigned to a domain based on a predefined ratio (e.g., 80/20

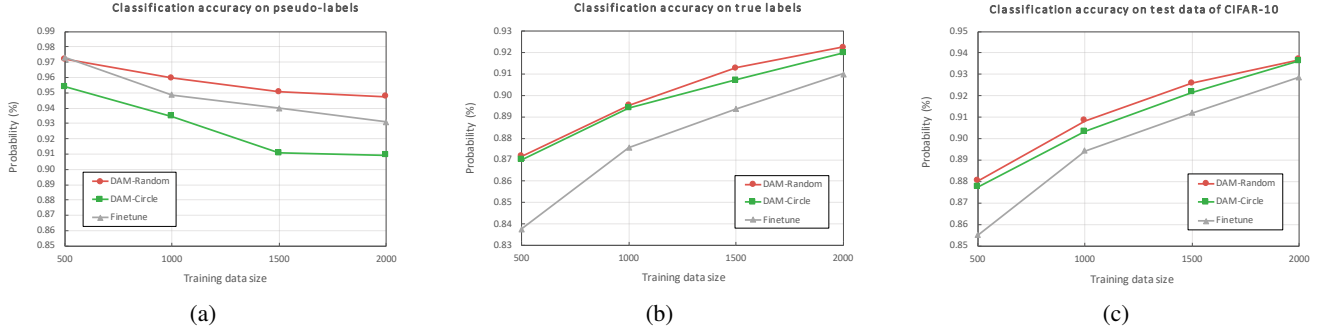


Figure 3: Training performance of DAM at various dataset sizes $|S_c|$ on CIFAR-10 using (a) pseudo-labels, (b) ground-truth labels, and (c) test data from CIFAR-10.

Table 3: Comparison of classification accuracy on CIFAR-10 and CIFAR-100 with baseline models such as Π -model (Laine and Aila 2016), PseudoLabel (Lee 2013), MixUp (Zhang et al. 2017), VAT (Miyato et al. 2018) MeanTeacher (Tarvainen and Valpola 2017), MixMatch (Berthelot et al. 2019b), EnAET (Wang et al. 2019), UDA (Xie et al. 2019), ReMixMatch (Berthelot et al. 2019a), and FixMatch (Sohn et al. 2020). The highest reported accuracies are used for baseline models. Top accuracies that fall within reported error margins are reported in bold.

CIFAR-10				CIFAR-100			
Method	250 labels	1000 labels	4000 labels	Method	2500 labels	5000 labels	10000 labels
Π -model	0.4903	0.6945	0.8296	Π -model	0.4323	-	0.6223
PseudoLabel	0.5119	0.7082	0.8390	PseudoLabel	0.4308	-	0.6398
MixUp	0.5349	0.7494	0.8705	Mean Teacher	0.4666	-	0.6441
VAT	0.6679	0.8172	0.8926	MixMatch	0.6043	-	0.7202
MeanTeacher	0.5739	0.8668	0.8989	EnAET	-	0.6817	0.7328
MixMatch	0.8979	0.9257	0.9382	UDA	0.6709	-	0.7575
ReMixMatch	0.9461	-	0.9541	ReMixMatch	0.7288	-	0.7753
FixMatch (RA)	0.9558	-	0.9579	FixMatch (RA)	0.7182	-	0.7752
LiDAM	0.8083	0.8904	0.9252	LiDAM	0.7350	0.7514	0.7678

split). This approach captures the intuition that multiple domains are spread across the each cluster, and so features can be best extracted after performing multiple local domain shifts in random directions. In the second approach, the distance to the cluster center is used to separate the two domains. This is defined by selecting points that fall within or outside an inscribed circle/sphere (i.e., the closest 80% are assigned to the source domain, the remaining 20% to target domain). The intuition behind this approach is that sample points nearest to cluster centroids will likely belong to a single domain; thus features are best extracted by shifting outward to domains in the periphery. As a baseline approach, we compare the performance of each of these experiments to a ResNet-50 model finetuned on S_s .

In Figure 3(a), we observe the performance of the DAM model at predicting psuedo-labels using both of these partitioning approaches on S_t . They key takeaway from this plot is that randomized domain shifts (DAM-Random) result in the extraction of more robust features compared to DAM-Circle and Finetune as the size of S_c increases and it's purity decreases (see Table 1). For comparison in Fig-

ure 3(b), we use the same partitions used in Figure 3(a), but instead train and predict on ground-truth labels. Here we can see that the model does not suffer from poor K -means psuedo-label assignment and instead leverages the true labels to progressively improve performance as more of it is provided. Finally, in Figure 3(c) we run this same experiment but test performance on the CIFAR-10 test partition. Overall, we conclude from these experiments that the DAM-Random approach performs better than the DAM-Circle approach, DAM is more accurate at predicting pseudo-labels with smaller sizes (e.g., 500) of S_c , and lastly DAM performs better than a finetuned ResNet-50 for learning essential features across multi-source domains. Therefore, we select this configuration and combine it with our iterative matching algorithm to test our full LiDAM framework.

CIFAR-10 Results We compare our technique with state-of-the art methods using varying amounts of ground-truth training data. We follow standard practice by randomly sampling 25, 100, and 400 labels per class. A full comparison of results is provided in Table 3. We provide the highest accuracies reported for each method by the original authors.

Top accuracies are indicated in bold, including those that fall within the reported error margins. Our approach is competitive but is outperformed in all labeling cases for CIFAR-10.

CIFAR-100 Results As seen in Table 3, our proposed method outperforms all other methods on 2500 labels and 5000 labels. On 2500 labels, we observe a 0.6% improvement compared to ReMixMatch and 1.68% improvement compared to FixMatch. Similar to the results on CIFAR-10, we outperform most other methods when using the minimal amount of data (2500 labels) even when other approaches use the all available data (10000 labels). Our method is also a top performer (within error margin) on 10000 labels.

Overall, our method defines a new state-of-the-art performance for CIFAR-100, but performs worse on CIFAR-10. Our main hypothesis for this discrepancy is that for the CIFAR-100 case, the number of samples in each class are small but the domain variance is large. This is likely an optimal scenario for LiDAM which primarily address such domain variance. On the other hand, CIFAR-10 contains fewer classes but a large number of samples per class. Therefore, there is an increased chance that the clusters identified by K -means will have accurately identified all samples across all domains, leading to less domain variance in the regions selected around each cluster centroid. Another point worth noting is that when using a large number of labels such as 10000 labels from CIFAR-100, as shown in Table 3), our method approaches the top accuracy but falls slightly short. One explanation for this small gap is our choice to use ResNet-50 as our backbone, in contrast to other methods. For example, both FixMatch and ReMixMatch use wide ResNet models (Huang et al. 2017) (e.g. Wide ResNet-28-2, Wide ResNet-28-10, etc.) which both perform better than ResNet-50 in their experiments. Our choice of using a ResNet-50 backbone is based on the availability of a pre-trained version of this network.

5 Conclusion

We have introduced LiDAM, a two-stage semi-supervised learning approach for deep image classification that combines deep domain adaptation for label initialization with a novel iterative algorithm for updating both labels and classifier parameters. To our knowledge, LiDAM is the first approach that utilizes localized domain adaptation to reduce intra-class domain variance for the purpose of boosting self-supervised learning. Our method achieves state-of-the-art performance on the CIFAR-100 dataset while achieving competitive performance on CIFAR-10. In future work, we will explore alternative backbone architectures and representation learning methods, including self-supervised approaches that train using pretext tasks. In addition, we will explore the integration of active learning approaches that selectively request labels for the most informative samples.

References

- Berthelot, D.; Carlini, N.; Cubuk, E. D.; Kurakin, A.; Sohn, K.; Zhang, H.; and Raffel, C. 2019a. Remixmatch: Semi-supervised learning with distribution alignment and augmentation anchoring. *arXiv preprint arXiv:1911.09785*.
- Berthelot, D.; Carlini, N.; Goodfellow, I.; Papernot, N.; Oliver, A.; and Raffel, C. A. 2019b. Mixmatch: A holistic approach to semi-supervised learning. In *Advances in Neural Information Processing Systems*, 5049–5059.
- Cao, Z.; Long, M.; Wang, J.; and Jordan, M. I. 2018. Partial transfer learning with selective adversarial networks. In *Proceedings of the IEEE Conference on Computer Vision and Pattern Recognition*, 2724–2732.
- Caron, M.; Bojanowski, P.; Joulin, A.; and Douze, M. 2018. Deep clustering for unsupervised learning of visual features. In *European Conference on Computer Vision*.
- Chen, T.; Kornblith, S.; Swersky, K.; Norouzi, M.; and Hinton, G. 2020. Big self-supervised models are strong semi-supervised learners. *arXiv preprint arXiv:2006.10029*.
- Ganin, Y., and Lempitsky, V. 2015. Unsupervised domain adaptation by backpropagation. In *International conference on machine learning*, 1180–1189.
- Garg, V. K., and Kalai, A. 2017. Supervising unsupervised learning.
- He, K.; Fan, H.; Wu, Y.; Xie, S.; and Girshick, R. 2019. Momentum contrast for unsupervised visual representation learning. *arXiv preprint arXiv:1911.05722*.
- Huang, G.; Liu, Z.; Van Der Maaten, L.; and Weinberger, K. Q. 2017. Densely connected convolutional networks. In *Proceedings of the IEEE conference on computer vision and pattern recognition*, 4700–4708.
- Krizhevsky, A.; Nair, V.; and Hinton, G. 2009. Cifar-10 and cifar-100 datasets. URL: <https://www.cs.toronto.edu/kriz/cifar.html> 6:1.
- Laine, S., and Aila, T. 2016. Temporal ensembling for semi-supervised learning. *arXiv preprint arXiv:1610.02242*.
- Lee, S.; Kim, D.; Kim, N.; and Jeong, S.-G. 2019. Drop to adapt: Learning discriminative features for unsupervised domain adaptation. In *The IEEE International Conference on Computer Vision (ICCV)*.
- Lee, D.-H. 2013. Pseudo-label: The simple and efficient semi-supervised learning method for deep neural networks. In *Workshop on challenges in representation learning, ICML*, volume 3.
- Mittal, S., and Sangwan, O. P. 2019. Big data analytics using machine learning techniques. In *2019 9th International Conference on Cloud Computing, Data Science Engineering (Confluence)*, 203–207.
- Miyato, T.; Maeda, S.-i.; Koyama, M.; and Ishii, S. 2018. Virtual adversarial training: a regularization method for supervised and semi-supervised learning. *IEEE transactions on pattern analysis and machine intelligence* 41(8):1979–1993.
- Sohn, K.; Berthelot, D.; Li, C.-L.; Zhang, Z.; Carlini, N.; Cubuk, E. D.; Kurakin, A.; Zhang, H.; and Raffel, C. 2020. Fixmatch: Simplifying semi-supervised learning with consistency and confidence. *arXiv preprint arXiv:2001.07685*.
- Tarvainen, A., and Valpola, H. 2017. Mean teachers are better role models: Weight-averaged consistency targets improve semi-supervised deep learning results. In *Advances in neural information processing systems*, 1195–1204.

- Wang, X.; Kihara, D.; Luo, J.; and Qi, G.-J. 2019. Enaet: Self-trained ensemble autoencoding transformations for semi-supervised learning. *arXiv preprint arXiv:1911.09265*.
- Xie, Q.; Dai, Z.; Hovy, E.; Luong, M.-T.; and Le, Q. V. 2019. Unsupervised data augmentation for consistency training. *arXiv preprint arXiv:1904.12848*.
- Yu, C.; Wang, J.; Chen, Y.; and Huang, M. 2019. Transfer learning with dynamic adversarial adaptation network. In *2019 IEEE International Conference on Data Mining (ICDM)*, 778–786. IEEE.
- Zhang, H.; Cisse, M.; Dauphin, Y. N.; and Lopez-Paz, D. 2017. mixup: Beyond empirical risk minimization. *arXiv preprint arXiv:1710.09412*.
- Zhao, H.; Zhang, S.; Wu, G.; Moura, J. M.; Costeira, J. P.; and Gordon, G. J. 2018. Adversarial multiple source domain adaptation. In *Advances in Neural Information Processing Systems*, 8568–8579.